Geochemical Perspectives Letters

Magnesiowüstite as a major nitrogen reservoir in Earth´s lowermost mantle

G. Rustioni[1], M. Wiedenbeck[2], N. Miyajima[1], A. Chanyshev[1], H. Keppler[1*]

https://doi.org/10.7185/geochemlet.2401

Abstract

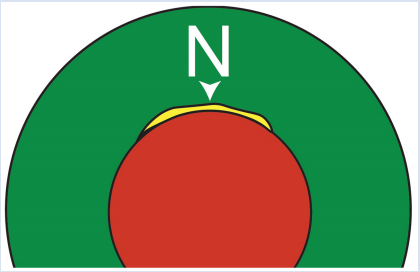

Ferropericlase (Mg,Fe)O is after bridgmanite the most abundant phase in the lower mantle. The ultralow velocity zones above the core-mantle boundary may contain very Fe-rich magnesiowüstite (Fe,Mg)O, possibly as result of the fractional crystallisation of a basal magma ocean. We have experimentally studied the solubility of nitrogen in the ferropericlase-magnesiowüstite solid solution series as function of iron content. Multi-anvil experiments were performed at 20–33 GPa and 1600–1800 °C in equilibrium with Fe metal. Nitrogen solubility increases from a few tens ppm (µg/g) for Mg-rich ferropericlase to more than 10 wt. % for nearly pure wüstite. Such high solubilities appear to be due to solid solution with NiAs-type FeN. Our data suggest that during fractional crystallisation of a magma ocean, the core-mantle boundary would have become extremely enriched with nitrogen, such that the deep mantle today could be the largest nitrogen reservoir on Earth. The often discussed "subchondritic N/C" ratio of the bulk silicate Earth may be an artefact of insufficient sampling of this deep reservoir.

Received 6 September 2023 | Accepted 4 December 2023 | Published 5 January 2024

Introduction

Nitrogen is the main constituent of Earth´s atmosphere. Nitrogen concentrations in the oceans, biomass and sediments and other near surface reservoirs are well constrained (Johnson and Goldblatt, 2015). The nitrogen abundance in the convecting upper mantle is also quite well known from measurements of $N/^{40}Ar$ ratios of MORB samples (Marty, 1995), which appear to be nearly unfractionated during partial melting and degassing (Keppler *et al.* 2022). If one considers the upper mantle to be representative of the entire bulk silicate Earth, these data would suggest that nitrogen on Earth is selectively depleted relative to carbon (Marty, 2012). This "subchondritic N/C ratio" has been extensively discussed and has often been used to constrain details of models for the early evolution of Earth (*e.g.*, Hirschmann, 2016; Li *et al.*, 2023).

There are, however, reasons to believe that the transition zone and lower mantle may be enriched in nitrogen, which would obviously call into question the concept of the "subchondritic N/C ratio" of the bulk Earth. Some samples from ocean island basalts have much higher $N/^{40}Ar$ ratios than MORB (Johnson and Goldblatt, 2015), which could hint at a deep seated N-rich reservoir. Moreover, experimental studies (Yoshioka *et al.*, 2018) suggest that in particular, the main minerals of the mantle transition zone, wadsleyite and ringwoodite, may store much more nitrogen than the minerals of the shallow mantle. Nitrogen solubility in minerals of the lower mantle, however, is poorly constrained. There are very few data on bridgmanite, the most abundant phase (Yoshioka *et al.*, 2018) and no data at all on ferropericlase, the second most abundant phase. In the present study we systematically investigated N solubility in the ferropericlase (Mg,Fe)O-magnesiowüstite (Fe,Mg)O solid solution series.

Methods

Ferropericlase or magnesiowüstite were synthesised together with other minerals (mostly bridgmanite) at 20–33 GPa and 1600–1800 °C in the presence of an N-rich fluid phase. Starting materials were oxide (SiO_2-MgO) hydroxide ($Mg(OH)_2$-$Al(OH)_3$) mixtures with bridgmanite ($MgSiO_3$) stoichiometry, sometimes containing up to 10 wt. % Al_2O_3. Metallic Fe was added to all charges either as powder or as 1mm thick disks to buffer oxygen fugacity near the Fe-FeO (iron wüstite) equilibrium, which is realistic for the lower mantle (Frost and McCammon, 2008). A N-rich fluid phase was generated by adding isotopically labelled ammonium nitrate $^{15}NH_4{}^{15}NO_3$ to the charge, which was sealed into Pt capsules. The weight ratio of metallic Fe to $^{15}NH_4{}^{15}NO_3$ and to the oxide-hydroxide mixture loaded in each capsule was about 5:1:2. Experiments up to 24 GPa were carried out in a conventional, Kawai-type multi-anvil apparatus. For experiments at higher pressures, a multi-anvil press of new design was used (Ishii *et al.*, 2016).

The samples recovered from high pressure experiments were embedded into epoxy resin, sectioned and polished. Nitrogen contents were measured both by electron microprobe

1. Bayerisches Geoinstitut, Universität Bayreuth, 95440 Bayreuth, Germany
2. GFZ Helmholtz-Zentrum Potsdam, Telegrafenberg, 14473 Potsdam, Germany
* Corresponding author (email: hans.keppler@uni-bayreuth.de)

(JEOL JXA-8200) and by SIMS (secondary ion microprobe analysis) using the Cameca 1280-HR instrument at GFZ Potsdam. For microprobe measurements, an acceleration voltage of 10 kV, beam current of 15 nA, and a 5 µm diameter defocused beam were used together with the following standards: Andradite and metallic iron for Fe, diopside for Mg, metallic platinum for Pt and boron nitride for N. For SIMS measurements, samples were coated with a 35 nm high purity gold layer. Measurements were carried out with a $^{16}O^-$ primary beam focused to a 10 µm diameter spot, 13 kV primary acceleration voltage, and 20–24 nA primary current. ^{15}N implanted forsterite was used as calibrant material. For further details, see Yoshioka *et al.* (2018).

In order to constrain the dissolution mechanism of nitrogen, the samples were also studied by Raman spectroscopy and by transmission electron microscopy (TEM). Raman spectra were measured with a Horiba Labram 800 HR-UV confocal spectrometer using the 514 nm line of a Coherent argon laser at 200 mW output power. TEM studies were carried out with a 200 kV FEI Titan instrument. Further experimental details are given in the Supplementary Information.

Nitrogen Solubility in Ferropericlase-Magnesiowüstite

A summary of all our high pressure experiments and analytical results is given in Tables S-1 and S-2. Figure 1 shows a typical run product. At pressures above 24 GPa, magnesiowüstite (or ferropericlase, depending on composition) coexists with bridgmanite and a metallic phase containing iron, as expected for the lower mantle. Other phases, in particular stishovite, are occasionally observed. In the majority of the experiments, most of the magnesiowüstite formed by the oxidation of a portion of the Fe metal that was initially added, which explains the rather Fe-rich compositions in most experiments. Measured nitrogen contents in the (Fe,Mg)O phase are shown in Figure 2 as function of FeO content. Nitrogen solubility in ferropericlase-magnesiowüstite increases from a few 10 µg/g for Mg-rich compositions to 18 wt. % (!) for the Fe end member. In general, the data from SIMS measurements define a consistent trend with only few outliers. The microprobe measurements (see also Table S-1) overlap with the SIMS data but most of them are displaced to lower values. This is likely due to degassing during the microprobe measurements, as the sample is heated in vacuum by the electron beam. Indeed, in a scan of the X-ray spectrum of the most N-rich samples, the nitrogen Kα line was clearly visible before the measurements, while it was invisible afterwards. Despite these analytical problems, we show the microprobe data here, as they provide an independent confirmation of the very high nitrogen contents obtained by SIMS. We cannot exclude that local heating may also occur during SIMS measurements, therefore our SIMS and microprobe measurements were never carried out at exactly the same locations. Some of the scatter seen in Figure 2 may also be related to variations in oxygen fugacity. The Fe metal in the runs is to a variable extent alloyed with Pt (see Table S-1) and this effect will shift the oxygen fugacity to values above the Fe-FeO buffer, which is expected to reduce nitrogen solubility in minerals (*e.g.*, Li *et al.*, 2013). The FeO contents in Figure 2 and Table S-1 were obtained by the usual standard procedures used for oxide and silicate analyses, *i.e.* all Fe was assumed to be Fe^{2+} and expressed as FeO. However, in reality (see the discussion below), some Fe is present as nitride in solid solution. For the most Fe-rich samples, this procedure produces totals (FeO + MgO + N) that may exceed 100 %. No attempt was made to correct for this.

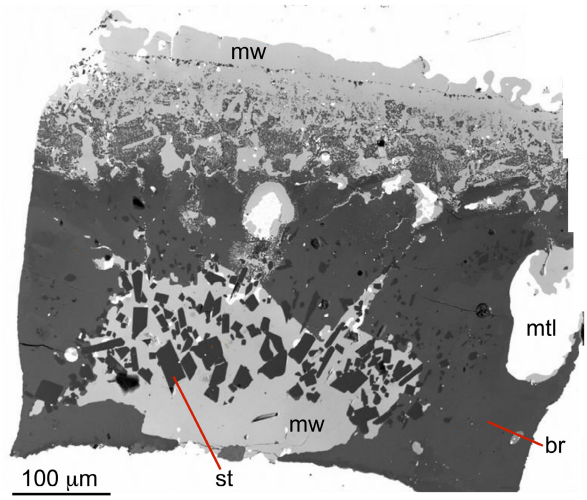

Figure 1 Backscatter electron image of sample BRG 22 (24 GPa, 1700 °C). Magnesiowüstite (mw) is light grey, Pt-bearing Fe metal (mtl) is white, bridgmanite (br) dark grey, and stishovite (st) nearly black.

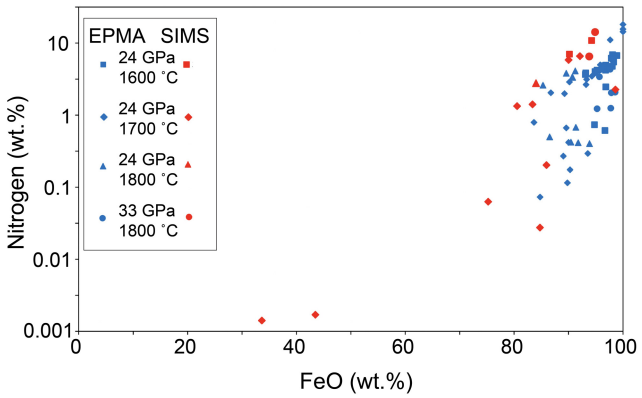

Figure 2 Nitrogen solubility in ferropericlase-magnesiowüstite solid solutions at Fe-FeO buffer conditions. Both data obtained by electron microprobe (EPMA) and by SIMS (secondary ion mass spectrometry) are shown. However, they were never measured at exactly the same spot, as nitrogen is likely lost during the measurements. Data at the same P,T conditions may be from several experiments, see Table S-1.

Nitrogen Substitution Mechanism in Ferropericlase-Magnesiowüstite

Wüstite is a non-stoichiometric phase, often written as $Fe_{1-x}O$. This is because some of the iron is present as Fe^{3+} (even at low oxygen fugacities), which is then charge compensated by Fe^{2+} vacancies. An alternative possibility of charge compensation for Fe^{3+} would be the substitution of Fe^{2+} by a univalent cation, such as Na^+. Indeed, samples of ferropericlase from the mantle can have elevated sodium contents (Brey *et al.*, 2004). Instead of Na^+, perhaps also the ammonium ion NH_4^+ could be incorporated into magnesiowüstite, which would be a possible mechanism for accommodating the exceptionally high nitrogen solubilities reported here. NH_4^+ would be easily detectable by Raman spectroscopy due to the N-H stretching vibrations near 3100 cm^{-1}. We therefore measured Raman spectra of some

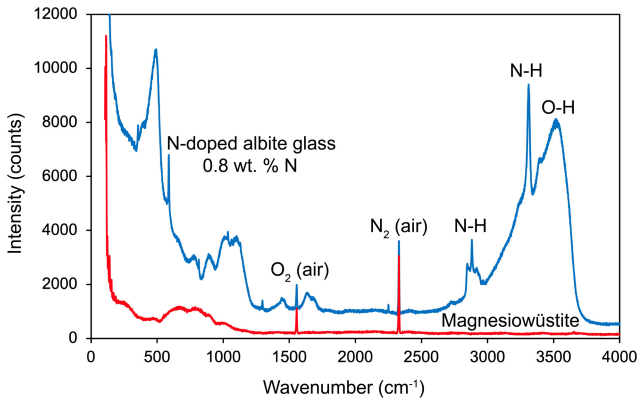

Figure 3 A comparison of the Raman spectrum of nitrogen-rich magnesiowüstite (run BRG 21) with the Raman spectrum of a reduced hydrous N-bearing albite glass with 0.8 wt. % N. The comparison clearly shows that N-H stretching vibrations would be detected in the magnesiowüstite, if the nitrogen were dissolved as ammonium ion or some other N-H species. Both spectra were acquired under the same conditions (2 times 50 s accumulation time, 200 mW output power, 514 nm argon laser).

of the most N-rich samples of magnesiowüstite. However, the spectra were completely featureless (Fig. 3). For pure magnesiowüstite (or ferropericlase), this is expected, as there is no Raman active vibrational mode in the rock salt structure. Significant ammonium concentrations should certainly be detectable by Raman spectroscopy. To demonstrate this, a hydrous albite glass with just 0.8 wt. % N was measured under the same conditions and clearly showed N-H bands (Fig. 3; see also Fig. S-1). Therefore, dissolution of nitrogen as NH_4^+ can be ruled out as the main substitution mechanism.

To further constrain the nitrogen substitution mechanism, some samples were studied by TEM (transmission electron microscopy). Electron diffraction patterns (Fig. 4a) showed that the magnesiowüstite with high N content is actually present in the form of single crystals without any phase impurities. High resolution images revealed the local presence of some nanoscale topotaxial spinel phase, which likely formed as exsolution during quenching and which is not associated with the high N contents (see Figs. S-2, S-3, and S-4). Figure 4b shows an ELNES (electron energy loss near edge structure) spectrum of a single crystal area of N-rich magnesiowüstite. The similarity of the fine structure of the N K-edge and the O K-edge suggest that N and O occur in the structure in the same coordination environment, *i.e.* N directly substitutes for O. In other words, the N-rich magnesiowüstite samples may be described as a solid solution of FeO with FeN. This is consistent with the description of NiAs-structured FeN that may be synthesised by direct reaction of N_2 with metallic iron above 17 GPa (Laniel *et al.*, 2018). The bonding in this FeN phase is probably largely metallic, such that it cannot be properly described with an ionic model. From a structural point of view, a significant miscibility between FeO and FeN is plausible, as the NiAs structure of FeN differs from the NaCl structure of FeO only by the stacking sequence of the densely packed anion layers. Indeed, extended solid solutions between structurally similar nitrides and oxides have been reported in the materials science literature (*e.g.*, Maeda *et al.*, 2005). The strong decrease of nitrogen solubility in magnesiowüstite with increasing Mg content may then be related to the transition from a mostly metallic to a dominantly ionic bonding environment in the crystal.

Nitrogen in the Lower Mantle and in the Ultralow Velocity Zones Above the Core

The molar fraction of Fe in ferropericlase in a pyrolitic lower mantle is likely between 0.1 and 0.3 depending on depth (*e.g.*, Irifune *et al.*, 2010; Muir and Brodholt, 2016). This translates into a composition of 16–43 wt. % FeO. As one may see from Figure 2, this corresponds to a nitrogen solubility in the range of a few tens μg/g. These numbers are comparable to the nitrogen solubility in bridgmanite (near 20 μg/g for Al-free bridgmanite; Yoshioka *et al.*, 2018). The estimates of Yoshioka *et al.* (2018) of the total nitrogen storage capacity of the lower mantle of 25 PAN (present atmospheric masses of nitrogen) would therefore require a significant upward revision. Even more interesting than the situation in the bulk lower mantle are the consequences of the data presented here for nitrogen sequestration just above the core-mantle boundary.

Numerous seismic studies have detected zones of ultralow seismic velocities (ULVZs) at various locations just above the core-mantle boundary (*e.g.*, Williams *et al.*, 1998; Cottaar and Romanowicz, 2012; Thorne *et al.*, 2013). Various hypotheses have been proposed to explain these features. Initially, it was widely believed that the presence of partial melt (*e.g.*, Williams *et al.*, 1998) might be responsible for the observed drop in seismic velocities. However, over the last decade, alternative models have received more support, which attribute these zones to chemical anomalies with very Fe-rich compositions containing near end member magnesiowüstite (Wicks *et al.*, 2010; Sun *et al.*, 2013; Brown *et al.*, 2015). Various models have been proposed for the origin of these Fe-enriched zones. They may perhaps be "sediments" of material exsolved from the liquid core (Buffett *et al.*, 2000) or consist of subducted banded iron formation (Dobson and Brodholt, 2005). An alternative idea is that these Fe-rich zones are remnants of the fractional crystallisation of a deep magma ocean, which caused increasingly Fe-rich minerals to be deposited at the core-mantle boundary during the Hadean (Labrosse *et al.*, 2007). If this latter model is correct, it would imply that these ULVZs may have concentrated most of the nitrogen that was originally dissolved in a magma ocean. This is so because the nitrogen solubility in magnesiowüstite measured here is one to two orders of magnitude higher than the nitrogen solubility in a silicate melt measured under comparable conditions of pressure, temperature, and oxygen fugacity (Roskosz *et al.*, 2013). While nitrogen is more or less incompatible in all other phases that may crystallise from a magma ocean (Li *et al.*, 2013; Yoshioka *et al.*, 2018), the data presented here suggest that it would be highly enriched in Fe-rich magnesiowüstite that would precipitate just above the core-mantle boundary.

A rough calculation may demonstrate that the ULVZs above the core-mantle boundary may very well be a major nitrogen reservoir in the solid Earth. For the following discussion, we ignore any nitrogen partitioning into the core, since for the very reducing conditions of Earth´s early accretion predicted by current models, N behaves as a lithophile element (*e.g.*, Speelmanns *et al.*, 2019). Enstatite chondrites, which may resemble most of the material that accreted to form the Earth, contain about 605 μg/g N, whereas the concentration of N in carbonaceous chondrites is on average more than twice as high (Johnson and Goldblatt, 2015). If the bulk N content of the accreting Earth was near that of enstatite chondrites, this would translate in a N_2 partial pressure of about 700 bar in a primordial atmosphere above a magma ocean (Yoshioka *et al.*, 2018). According to Libourel *et al.* (2003), N_2 solubility in a

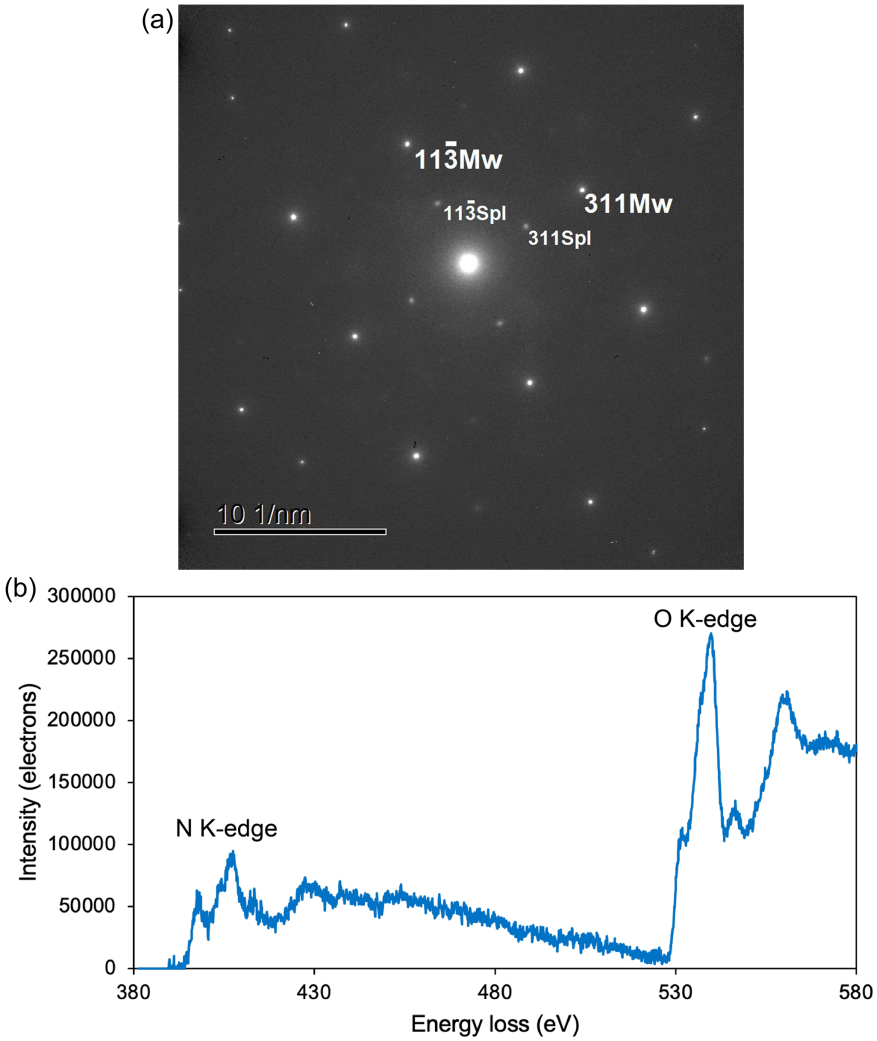

Figure 4 Transmission electron microscopic data on N-bearing magnesiowüstite. **(a)** Selected area electron diffraction (SAED) pattern of a sample showing that the investigated area is a single crystal of cubic magnesiowüstite (Mw) without phase impurities. Weaker diffraction spots of a spinel phase (Spl) are also visible in a complete topotaxy, with a-axis (Mw) // a-axis (Spl), indicating that this phase likely formed by exsolution during quenching. **(b)** ELNES (energy loss near edge structure) spectrum of N-bearing magnesiowüstite. The data show that nitrogen is contained in the lattice of the crystal and the environment of N and O are similar.

basaltic melt is about 0.06 (µg/g)/bar at conditions near the iron wüstite buffer; it may become even larger at more reducing conditions and at high H_2O fugacities (Li *et al.*, 2015; Bernadou *et al.*, 2021). If one accepts the rather conservative solubility of 0.06 (µg/g)/bar, this would imply that the magma ocean in equilibrium with the primordial atmosphere may have contained 42 µg/g N, equivalent to $1.70 \cdot 10^{20}$ kg. If only 20 % of the mass of this magma ocean had been trapped somewhere deep in the mantle during progressive crystallisation, as suggested by Labrosse *et al.* (2007), it would contain a N reservoir of $3.4 \cdot 10^{19}$ kg, more than 8 PAN (present atmospheric masses of nitrogen). Upon crystallisation of this deep magma reservoir, both nitrogen and Fe would become enriched in the residual melt, ultimately leading to the precipitation of very Fe-rich magnesiowüstite that is presently contained in the ULVZs. If one assumes that these ULVZs are about 15 km thick (*e.g.*, Cottaar and Romanowicz, 2012) and cover approximately 10 % of the core-mantle boundary, they would contain 13 wt. % N, if all the N in the deep melt reservoir were sequestered in there. This number is quite consistent with the measured solubilities of N in magnesiowüstite.

Is the "Subchondritic N/C Ratio of the Earth" Real?

Maybe not. The data presented here show that a very small and probably very poorly sampled reservoir near the core-mantle boundary could contain enough nitrogen to make the roughly one order of magnitude (Marty, 2012) apparent depletion of N relative to C in the bulk Earth disappear. This further emphasises a conclusion reached already by Yoshioka *et al.* (2018) that the solubilities of N in ordinary minerals of the transition zone or the lower mantle are large enough that the deep mantle could have sequestered a large fraction of Earth´s nitrogen during magma ocean crystallisation. On the other hand, while the N content of the depleted MORB-source mantle (*e.g.* Marty, 1995) is very well constrained, data on the deep mantle are sparse. While many ocean island basalts do indeed have $N/^{40}Ar$ ratios similar to MORB, there are also some samples with much higher values (Johnson and Goldblatt, 2015) that may hint at a deep hidden reservoir. Based on our current state of knowledge, the bulk N/C ratio of the Earth appears to be rather uncertain and this ratio should not be used as a parameter for constraining

planetary accretion models (*e.g.*, Hirschmann, 2016; Li *et al.*, 2023).

Acknowledgements

Takahiro Yoshioka kindly carried out some of the early experiments in this project. We thank Dorothea Wiesner for the preparation of the TEM thin foil by FIB. This work was supported by Deutsche Forschungsgemeinschaft (DFG; grant Ke 501/13-2 to HK). Comments by Raúl Fonseca and reviews by Mathieu Roskosz and by an anonymous referee helped to improve the manuscript.

Editor: Raúl O.C. Fonseca

Additional Information

Supplementary Information accompanies this letter at https://www.geochemicalperspectivesletters.org/article2401.

Cite this letter as: Rustioni, G., Wiedenbeck, M., Miyajima, N., Chanyshev, A., Keppler, H. (2024) Magnesiowüstite as a major nitrogen reservoir in Earth´s lowermost mantle. *Geochem. Persp. Let.* 28, 43–47. https://doi.org/10.7185/geochemlet.2401

References

Bernadou, F., Gaillard, F., Füri, E., Marrocchi, Y., Slodczyk, A. (2021) Nitrogen solubility in basaltic silicate melt - Implications for degassing processes. *Chemical Geology* 573, 120192. https://doi.org/10.1016/j.chemgeo.2021.120192.

Brey, G.P., Bulatov, V., Girnisc, A., Harris, J.W., Stachel, T. (2004) Ferropericlase—a lower mantle phase in the upper mantle. *Lithos* 77, 655–663. https://doi.org/10.1016/j.lithos.2004.03.013.

Brown, S. P., Thorne, M. S., Miyagi, L., Rost, S. (2015) A compositional origin to ultralow-velocity zones. *Geophysical Research Letters* 42. https://doi.org/10.1002/2014GL062097.

Buffett, B.A., Garnero, E.J., Jeanloz, R. (2000) Sediments at the top of Earth´s core. *Science* 290, 1338–1342. https://doi.org/10.1126/science.290.5495.1338.

Cottaar, S., Romanowicz, B. (2012) An unusually large ULVZ at the base of the mantle near Hawaii. *Earth and Planetary Science Letters* 355–356, 213–222. https://doi.org/10.1016/j.epsl.2012.09.005.

Dobson, D.P., Brodholt, J.P. (2005) Subducted banded iron formations as a source of ultralow-velocity zones at the core-mantle boundary. *Nature* 434, 371–374. https://doi.org/10.1038/nature03430.

Frost, D., McCammon, C. (2008) The redox state of Earth's mantle. *Annual Review of Earth and Planetary Sciences* 36, 389–420. https://doi.org/10.1146/annurev.earth.36.031207.124322.

Hirschmann, M.M. (2016) Constraints on the early delivery and fractionation of Earth's major volatiles from C/H, C/N, and C/S ratios. *American Mineralogist* 101, 540–553. https://doi.org/10.2138/am-2016-5452.

Irifune, T., Shinmei, T., McCammon, C.A., Miyajima, N., Rubie, D.C., Frost, D.J. (2010) Iron partitioning and density changes of pyrolite in Earth's lower mantle. *Science* 327, 193–195. https://doi.org/10.1126/science.1181443.

Ishii, T., Shi, L., Huang, R., Tsujino, N., Druzhbin, D., Myhill, R., Li, Y., Wang, L., Yamamoto, T., Miyajima, N., Kawazoe, T., Nishiyama, N., Higo, Y., Tange, Y., Katsura, T. (2016) Generation of pressures over 40 GPa using Kawai-type multi-anvil apparatus with tungsten carbide anvils. *Reviews of Scientific Instruments* 87, 024501. https://doi.org/10.1063/1.4941716.

Johnson, B., Goldblatt, C. (2015) The nitrogen budget of Earth. *Earth-Science Reviews* 148, 150–173. https://doi.org/10.1016/j.earscirev.2015.05.006.

Keppler, H., Cialdella, L., Couffignal, F., Wiedenbeck, M. (2022) The solubility of N_2 in silicate melts and nitrogen partitioning between upper mantle minerals and basalt. *Contributions to Mineralogy and Petrology* 177, 83. https://doi.org/10.1007/s00410-022-01948-z.

Labrosse, S., Hernlund, J.W., Coltice, N. (2007) A crystallizing dense magma ocean at the base of the Earth's mantle. *Nature* 450, 866–869. https://doi.org/10.1038/nature06355.

Laniel, D., Dewaele, A., Anzellini, S., Guignot, N. (2018) Study of the iron nitride FeN into the megabar regime. *Journal of Alloys and Compounds* 733, 53–58. https://doi.org/10.1016/j.jallcom.2017.10.267.

Li, Y., Wiedenbeck, M., Shcheka, S., Keppler, H. (2013) Nitrogen solubility in upper mantle minerals. *Earth and Planetary Science Letters* 377, 311–323. https://doi.org/10.1016/j.epsl.2013.07.013.

Li, Y., Huang, R., Wiedenbeck, M., Keppler (2015) Nitrogen distribution between aqueous fluids and silicate melts. *Earth and Planetary Science Letters* 411, 218–228. https://doi.org/10.1016/j.epsl.2014.11.050.

Li, Y., Wiedenbeck, M., Monteleone, B., Dasgupta, R., Costin, G., Gao, Z., Lu, W (2023) Nitrogen and carbon fractionation in planetary magma oceans and origin of the superchondritic C/N ratio in the bulk silicate Earth. *Earth and Planetary Science Letters* 605, 118032. https://doi.org/10.1016/j.epsl.2023.118032.

Libourel, G., Marty, B., Humbert, F. (2003) Nitrogen solubility in basaltic melt. Part I. Effect of oxygen fugacity. *Geochimica et Cosmochimica Acta* 67, 4123–4135. https://doi.org/10.1016/S0016-7037(03)00259-X.

Maeda, K., Takata, T., Hara, M., Saito, N., Inoue, Y., Kobayashi, H., Domen, K. (2005) GaN:ZnO solid solution as a photocatalyst for visible-light-driven overall water splitting. *Journal of the American Chemical Society* 127, 8286–8287. https://doi.org/10.1021/ja0518777

Marty, B. (1995) Nitrogen content of the mantle inferred from N_2–Ar correlation in oceanic basalts. *Nature* 377, 326–329. https://doi.org/10.1038/377326a0.

Marty, B. (2012) The origins and concentrations of water, carbon, nitrogen and noble gases on Earth. *Earth and Planetary Science Letters* 313, 56–66. https://doi.org/10.1016/j.epsl.2011.10.040.

Muir, J.M.R., Brodholt, J.P. (2016) Ferrous iron partitioning in the lower mantle. *Physics of the Earth and Planetary Interiors* 257, 12–17. https://doi.org/10.1016/j.pepi.2016.05.008.

Roskosz, M., Bouhifd, M., Jephcoat, A., Marty, B., Mysen, B. (2013) Nitrogen solubility in molten metal and silicate at high pressure and temperature. *Geochimica et Cosmochimica Acta* 121, 15–28. https://doi.org/10.1016/j.gca.2013.07.007.

Speelmanns, I.M., Schmidt, M.W., Liebske, C. (2019) The almost lithophile character of nitrogen during core formation. *Earth and Planetary Science Letters* 510, 186–197. https://doi.org/10.1016/j.epsl.2019.01.004

Sun, D., Helmberger, D.V., Jackson, J.M., Clayton, R.W., Bower, D.J. (2013) Rolling hills on the core–mantle boundary. *Earth and Planetary Science Letters* 361, 333–342. https://doi.org/10.1016/j.epsl.2012.10.027.

Thorne, M.S., Garnero, E.J., Jahnke, G., Igel, H., McNamara, A.K. (2013) Mega ultra low velocity zone and mantle flow. *Earth and Planetary Science Letters* 364, 59–67. https://doi.org/10.1016/j.epsl.2012.12.034.

Yoshioka, T., Wiedenbeck, M., Shcheka, S., Keppler, H. (2018) Nitrogen solubility in the deep mantle and the origin of Earth's primordial nitrogen budget. *Earth and Planetary Science Letters* 488, 134–143. https://doi.org/10.1016/j.epsl.2018.02.021.

Wicks, J.K., Jackson, J.M., Sturhahn, W. (2010) Very low sound velocities in iron-rich (Mg,Fe)O: Implications for the core-mantle boundary region. *Geophysical Research Letters* 37, L15304. https://doi.org/10.1029/2010GL043689.

Williams, Q., Revenaugh, J., Garnero, E. (1998) A correlation between ultra-low basal velocities in the mantle and hot spots. *Science* 281, 546–554. https://doi.org/10.1126/science.281.5376.546.

Geochemical Perspectives Letters

Magnesiowüstite as a major nitrogen reservoir in Earth´s lowermost mantle

G. Rustioni, M. Wiedenbeck, N. Miyajima, A. Chanyshev, H. Keppler

Supplementary Information

The Supplementary Information includes:

- Methods Supplementary Information
- Figures S-1 to S-4
- Tables S-1 and S-2

Methods Supplementary Information

Raman spectroscopy

Raman spectra were measured at Bayerisches Geoinstitut, Bayreuth using a confocal Horiba Labram 800 HR UV spectrometer with an 1800 mm^{-1} grating, a Peltier-cooled CCD detector, and a 50 x objective. Spectral resolution was about 3 cm^{-1}. The 514 nm line of an argon laser with 200 mW output power as used for excitation. Spectra were acquired with 2 x 5 s or 2 x 50 s accumulation time. The sensitivity of Raman spectrometry for the ammonium ion and other N-H species is demonstrated in Figure S-1.

Transmission electron microscopy (TEM)

TEM studies, combined with energy-dispersive X-ray spectroscopy (EDS, Bruker-Quantax system) and electron energy-loss spectroscopy (EELS, Gatan GIF Quantum SE), were carried out with a 200 kV FEI Titan G2 80-200 S/TEM instrument. TEM thin foils were prepared using a FEI Scios focused ion beam instrument. The foils were investigated by selected area electron diffraction and conventional bright-field and dark-field imaging in TEM mode. The ELNES (energy loss near edge structure) spectrum of a single-crystal area of N-rich magnesiowüstite was measured in a scanning TEM mode. The conditions were convergent semi-angle (alpha) 10 mrad, collection semi-angle (beta) 17 mrad, and 200 s integration time (2 s exposure x 100 times). Figures S-2, S-3, and S-4 show additional evidence for the homogeneous distribution of N in single crystals of magnesiowüstite. The EDS elemental maps (Fig. S-3) were acquired for 420 s with the same beam conditions in the scanning TEM mode. The resolution of the pixel size is 3 nm in the 256 x 256-pixel map.

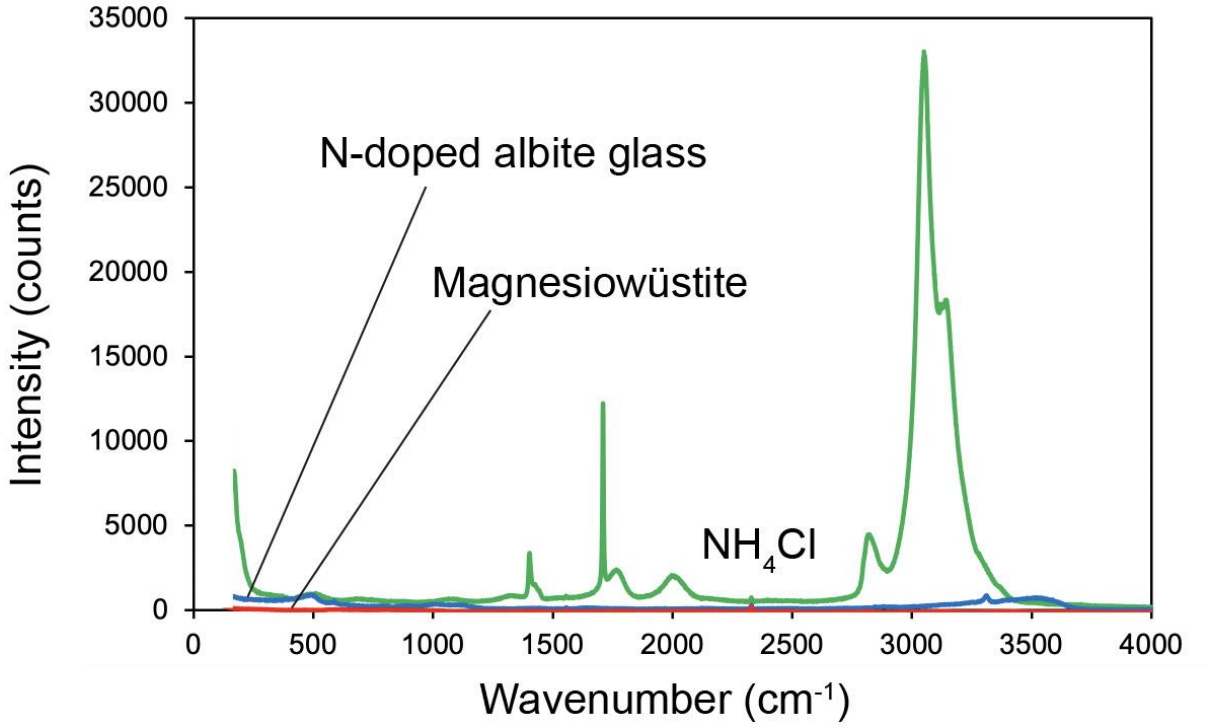

Figure S-1 A demonstration of the sensitivity of Raman spectroscopy for the ammonium ion and other N-H species. Raman spectra of pure NH_4Cl, a N-bearing hydrous albite glass with 0.8 wt. % of N and a N-rich magnesiowüstite sample were measured under the same conditions (2 times 5 s accumulation time, 200 mW output power, 514 nm Ar laser). Note that the accumulation time here is 10 times lower than for the spectra in Figure 3 of the main text, the magnesiowüstite and albite glass samples are the same. Nevertheless, even after 5 s, the N-H stretching band near 3300 cm^{-1} is still seen in the albite glass spectrum (see also Fig. 3 in the main text). The intensity roughly scales with the N-H stretching band system from 2800 – 3300 cm^{-1} in NH_4Cl as expected from the difference in nitrogen concentration.

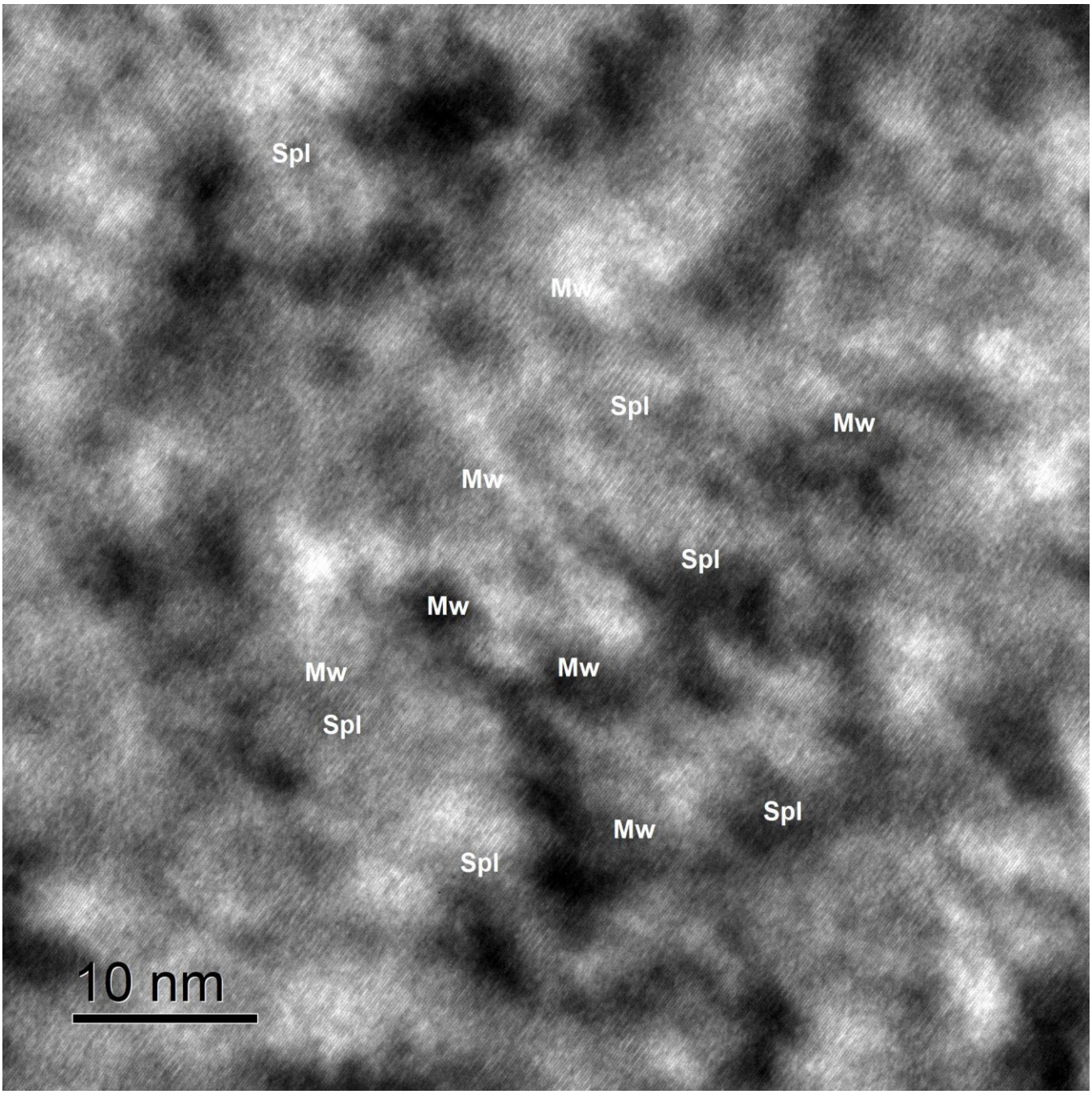

Figure S-2 High-resolution lattice TEM image of a single crystal of nitrogen-rich magnesiowüstite (Mw) with an exsolved spinel phase (Spl). The {220} fringes of 0.15 nm (Mw) and 0.30 nm (Spl) are visible. The image shows that no foreign N-bearing phases are present.

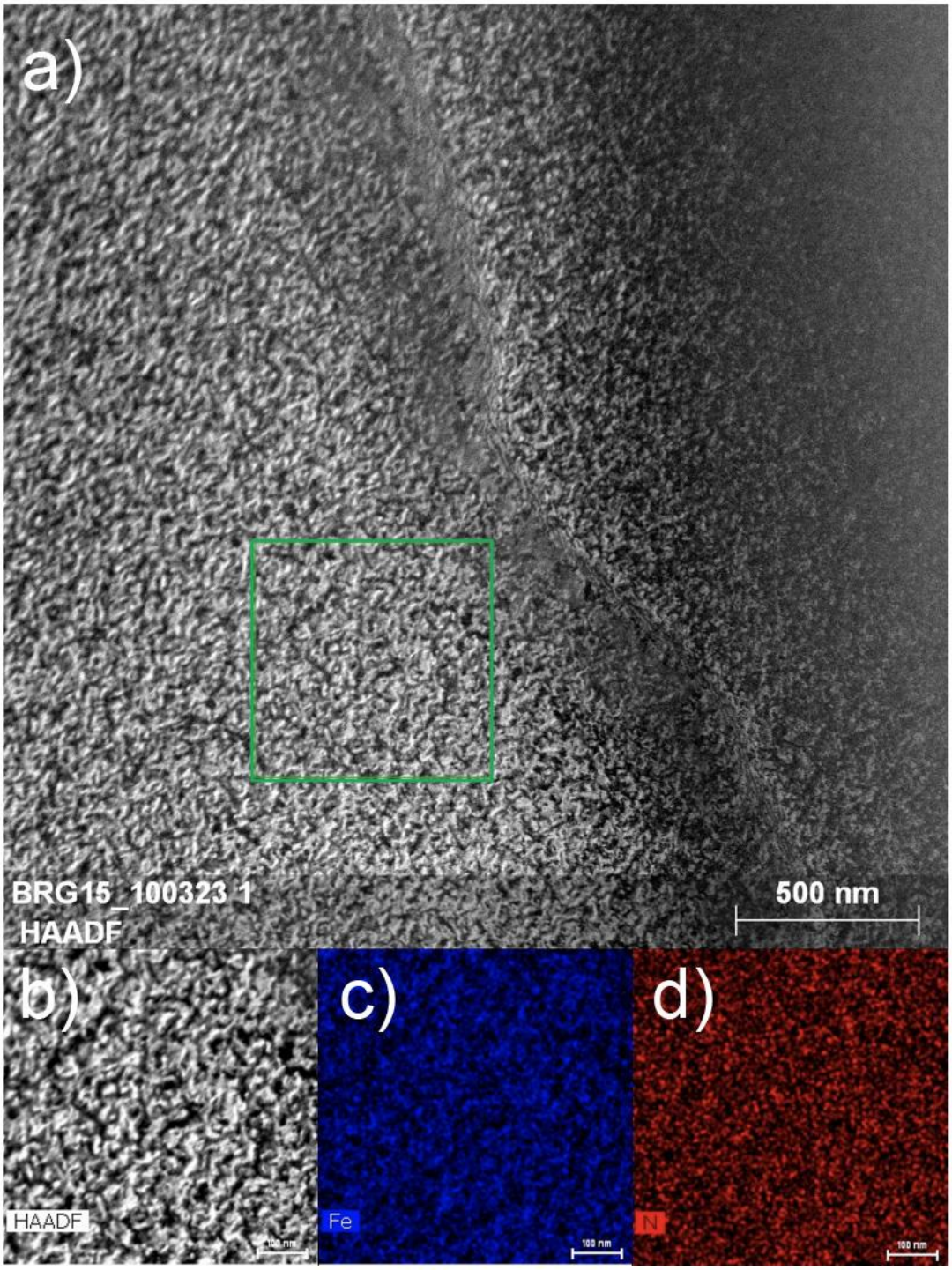

Figure S-3 **(a)** High-angle annular dark field (HAADF)-STEM image of a single crystal of N-rich magnesiowüstite. **(b)** The corresponding area (green square in the image a) of Fe and N elemental maps as seen by energy-dispersive X-ray spectroscopy (EDS; image **c and d**). Variations in local Fe-K and N-K X-ray intensity are within the range expected from counting statistics for a chemically homogeneous sample.

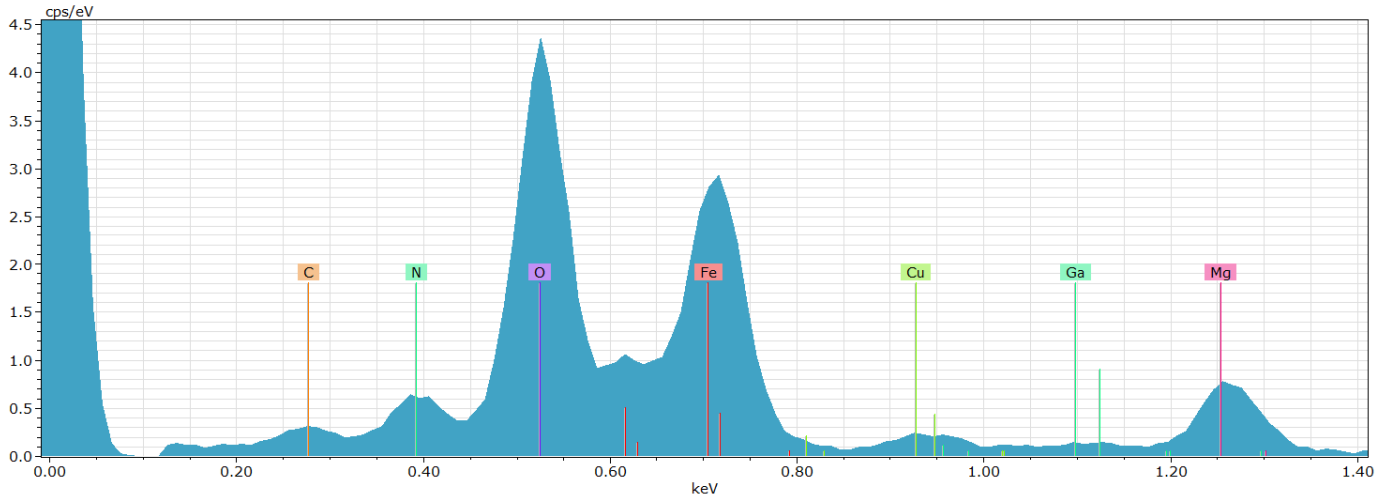

Figure S-4 A representative EDS spectrum (up to 1.4 keV) produced from part of the region shown in Figure S-3b. The peak of the N K-line is clearly detected.

Table S-1 Summary of high-pressure experiments on nitrogen solubility in ferropericlase - magnesiowüstite.

Run no	P (GPa)	T (˚C)	Duration (hrs)	Phases	Fe (wt. %) in metal	FeO (wt. %) in fp	N (wt. %) EPMA	N (wt. %) SIMS
MAJ01*	20	1700	5	maj, rw, fp, st, mtl	5.8 – 8.9	85.0 – 86.7	0.025 – 0.13	0.19 – 0.30
S7160	24	1600	1	br,fp, mtl	26.0 – 30.2	93.2 – 98.2	4.0 – 6.0	10.8
S7124	24	1600	3	br, fp, mtl	20.4 – 41.5	96.9 – 99.0	2.0 – 7.0	-
H4804	24	1600	3	br, fp, mtl	74.6 – 75.8	90.2	-	6.9
BRG01	24	1700	1.5	br, fp, st	4.9 – 12.7	89.1 – 93.5	0.11 – 0.42	-
BRG03*	24	1700	6	br, rw, fp, st	-	79.9	0.04 – 0.14	-
BRG05	24	1700	5.5	br, fp, st, mtl	6.6 – 8.8	80.6 – 83.4	-	1.3 – 1.4
BRG14*	24	1700	6.5	br, fp, st, mtl	3.3 – 9.1	85.0 – 89.5	0.066 – 0.28	-
BRG15	24	1700	6	br, fp, st, mtl	9.1 – 9.5	94.3 – 95.8	3.5 – 5.0	-
BRG21	24	1700	5	br, fp, mtl	97.8 – 98.6	83.7 – 100	0.17 – 18.1	0.2 – 2.3
BRG22	24	1700	6	br, fp, st, mtl	23.5 – 26.3	89.2 – 93.3	2.0 – 3.1	5.9 – 6.6
FPER01	24	1700	6	br, fp, mtl	75.9 – 90.1	26.8 – 97.7	< DL – 11.0	0.0014 – 0.063
BRG23	24	1800	6	br, fp, mtl	61.4 – 63.7	84.0 – 93.8	0.42 – 0.68	2.8
BRG24	24	1800	6	br, fp,mtl	12.6 – 13.0	85.3 – 91.3	2.6 – 4.1	-
IBRG01	33	1800	2	br, fp, st, mtl	41.0 – 42.1	93.7 – 98.6	1.2 – 4.3	6.5 – 14.0

EPMA (Electron microprobe) and SIMS (secondary ion mass spectrometry) measurements were not carried out at the same spot, because of the nitrogen loss associated with the measurements. In general, for each sample only one or two measurements were carried out by SIMS and about five by electron microprobe. FeO concentrations in the ferropericlase-magnesiowüstite solid solutions are microprobe data from the same spots as the nitrogen measurements. *Runs marked with a star contain either no metal phase at all or the metal phase is nearly pure Pt with little Fe, such that oxygen fugacity likely as not buffered near the Fe-FeO equilibrium; results from these three runs are therefore not plotted in Figure 2. Abbreviations: br = bridgmanite, fp = ferropericlase or magnesiowüstite, depending on FeO content, maj = majorite, rw = ringwoodite, st = stishovite, mtl = Fe-Pt metal alloy, DL = detection limit.

Table S-2 SIMS data on nitrogen solubility in ferropericlase - magnesiowüstite.

Sample	P	T (˚C)	SiO_2 (wt. %)	Al_2O_3 (wt. %)	MgO (wt. %)	FeO (wt. %)	Sum oxides (wt. %)	^{15}N (wt. %)
MAJ01_a	20	1700	0.91	0.34	7.83	85.94	95.02	0.30
MAJ01_b	20	1700	0.98	0.24	9.55	85.00	95.77	0.19
S7160	24	1600	0.05	0.05	5.13	94.30	99.5	10.77
H4804	24	1600	0.01	0.09	10.03	90.24	100.4	6.94
BRG05_a	24	1700	0.24	0.01	14.70	83.41	98.4	1.41
BRG05_b	24	1700	0.25	0.00	15.44	80.56	96.2	1.34
BRG21_a	24	1700	0.03	0.12	1.12	98.65	99.9	2.26
BRG21_b	24	1700	0.00	0.33	13.28	85.96	99.6	0.20
BRG22_a	24	1700	0.02	0.21	9.16	90.01	99.4	5.86
BRG22_b	24	1700	0.03	0.15	6.27	92.12	98.6	6.58
BRG23	24	1800	2.37	0.03	16.52	84.03	102.9	2.79
IBRG01_a	33	1800	0.00	0.33	3.05	93.86	97.2	6.48
IBRG01_b	33	1800	0.02	0.11	3.48	94.93	98.5	14.05
FPer01_a	24	1700	0.15	n.m.	24.91	75.29	100.3	0.063
FPer01_b	24	1700	0.16	n.m.	15.13	84.76	100.0	0.027
FPer01_c	24	1700	0.002	n.m.	66.69	33.66	100.3	0.0014
FPer01_d	24	1700	0.0271	n.m	56.76	43.5	100.3	0.0017

^{15}N concentrations were measured by SIMS (secondary ion mass spectrometry). The data shown are measurements from one single spot each, such that no meaningful standard deviation can be given. The major elements were measured by electron microprobe at a spot close to the SIMS measurement. n.m. = not measured.